Uncooled Terahertz real-time imaging 2D arrays developed at LETI: present status and perspectives

François Simoens*[a], Jérôme Meilhan[a], Laurent Dussopt[a], Jean-Alain Nicolas[a], Nicolas Monnier [a], Gilles Sicard[a], Alexandre Siligaris[a], Bruno Hiberty[b]
[a] CEA-Leti, Minatec Campus, Université Grenoble Alpes, 17, Rue des Martyrs, 38054 Grenoble, France. [b]i2S, F33600 Pessac, France.

ABSTRACT

As for other imaging sensor markets, whatever is the technology, the commercial spread of terahertz (THz) cameras has to fulfil simultaneously the criteria of high sensitivity and low cost and SWAP (size, weight and power). Monolithic silicon-based 2D sensors integrated in uncooled THz real-time cameras are good candidates to meet these requirements.

Over the past decade, LETI has been studying and developing such arrays with two complimentary technological approaches, i.e. antenna-coupled silicon bolometers and CMOS Field Effect Transistors (FET), both being compatible to standard silicon microelectronics processes. LETI has leveraged its know-how in thermal infrared bolometer sensors in developing a proprietary architecture for THz sensing. High technological maturity has been achieved as illustrated by the demonstration of fast scanning of large field of view and the recent birth of a commercial camera. In the FET-based THz field, recent works have been focused on innovative CMOS read-out-integrated circuit designs. The studied architectures take advantage of the large pixel pitch to enhance the flexibility and the sensitivity: an embedded in-pixel configurable signal processing chain dramatically reduces the noise. Video sequences at 100 frames per second using our 31x31 pixels 2D Focal Plane Arrays (FPA) have been achieved.

The authors describe the present status of these developments and perspectives of performance evolutions are discussed. Several experimental imaging tests are also presented in order to illustrate the capabilities of these arrays to address industrial applications such as non-destructive testing (NDT), security or quality control of food.

Keywords: antenna-coupled bolometer terahertz array, antenna-coupled Field Effect Transistor terahertz array, terahertz real-time imaging, terahertz uncooled 2D camera.

1. INTRODUCTION

The spread of THz imaging applications would be greatly increased by the availability of affordable, compact, easy-to-use and highly-sensitive cameras. These cameras would integrate large-format (many pixels) focal plane arrays and, like any digital camera, they would operate in video-mode recording streams in real-time without the need for raster scanning.

Currently, more and more uncooled terahertz (THz) real-time imaging cameras integrating two-dimensional (2D) sensors are being developed and commercialized [1]. The limited sensitivity which results from uncooled operation is overcome by implementing active imaging configuration: in active systems, an artificial light source –or several sources- is used to illuminate the scene and the image is formed by detecting the back-scattered and reflected radiation. On the other hand, such cameras can fulfil the criteria of low cost and low SWAP (Size, Weight, And Power) that any commercial camera has to target in order to be widely applied.

Micro- and Nanotechnology Sensors, Systems, and Applications IX, edited by Thomas George, Achyut K. Dutta, M. Saif Islam, Proc. of SPIE Vol. 10194, 101942N · © 2017 SPIE
CCC code: 0277-786X/17/$18 · doi: 10.1117/12.2263221

Table 1. List of commercial uncooled THz 2D cameras

Camera - Company	2D sensors	Spectral bandwidth, frame rate Optics
TZCAM by i2S [1]	320x240 amorphous silicon (a-Si) microbolometer array, pitch = 50µm LETI is the provider of the sensor	0.6-3THz, 25fps F/0.8, 50mm focal length
IR/V-T0831 by NEC [2], *NEC has decided to discontinue production*	320x240 oxide-vanadium (VOx) microbolometer array, pitch = 23.5µm	1-7THz, 500fps F/1, 28.2mm focal length
MICROXCAM-384I-THZ by INO [3]	384x288 oxide-vanadium (VOx) microbolometer array, pitch = 35µm	70–3.189 µm (4.25–0.094 THz), 50fps fast (F/0.9) or ultra-fast (F/0.7) HRFZ-Si, 44 mm focal length
TicMOS-1px by Tic-Wave [4]	100x100 field-effect-transistors array	0.3-1.3THz, 500fps No optics
Tera-256 / 1024 / 2056 by Terasense [5]	16x16 / 32x32 / 64x64 field-effect-transistors array, pitch = 1.5mm	10 GHz — 0.7 THz No optics
Pyrocam IV Beam Profiling Camera by Ophir Photonics [6]	320x240 pyroelectric array, pitch= 80µm	[13-355nm, 1.06-3000µm = f(window assembly with A/R coating)], 100 fps No optics
OpenView by Nethis [7]	256x320 pitch 170µm / 512x640 pitch 80µm, based on THz to IR converter	0.1 – 3000 µm, 1kfps No optics

When only direct detection by the pixel array is considered –that ensures smallest latency between frames-, array formats listed in table 1 vary from 16x16 to 384x288 pixels, the largest and most sensitive ones being provided by micro-bolometer technology-based sensors (refer to chapter 6. Components for terahertz imaging of [8]). Since the 90's, LETI [9] is developing such technology applied to thermal infrared (IR) imaging, which is now commercialized by the French company Ulis, a world leader in the IR array market. For almost one decade, LETI has been working on tailoring its proprietary bolometer technology for optimized THz arrays. The patented bolometer pixel array can be collectively processed above CMOS Read-Out Integrated Circuits (ROICs) with standard silicon technology, resulting in monolithic sensors delivering a video output. High technological maturity has been achieved as illustrated by the demonstration of world-state of the art sensitivity and fast scanning of large field of view. This technological maturity has lead up to the birth of a commercial THz camera listed in the previous table.

Complementary to the bolometric approach, LETI is studying and developing THz arrays based on CMOS Field Effect Transistors (FET), either in direct or heterodyne detection [10]. Researches for direct detection in FETs are currently focused on innovative read-out-integrated circuit designs. The studied architectures take advantage of the large pixel pitch to enhance the flexibility and the sensitivity: an embedded in-pixel configurable signal processing chain dramatically reduces the noise. Video sequences at 100 frames per second using our 31x31 pixels prototyped 2D FPAs have been achieved. One alternative development is heterodyne detection based on LETI's strong experience in millimeter-wave transceivers for high data-rate wireless communications. Single pixel heterodyne source and detector have been designed and prototyped with preliminary demonstrations of highly sensitive raster scanning THz imaging.

This paper will present the current results of these developments that cover complementary uncooled technological approaches for THz active real-time imaging.

2. MICROBOLOMETER ARRAYS TECHNOLOGY

2.1 Bolometer-based THz sensor architecture comparison

In contrast to thermal infrared microbolometers and THz microbolometers proposed by other laboratories, LETI's patented pixel architecture separates the THz radiation absorber design (antennas with resistive loads) and the thermometer (amorphous silicon film). Each pixel combines a suspended membrane with a double bow-tie antenna coupling the incident wave to resistive loads (Fig. 1 left) [11] [12]. The longer bowtie antenna located on the microbridge, named "DC (direct coupling) Antenna", is directly excited by the incident THz wave whose polarization is aligned along the axis of this antenna. A sub-antenna is used to couple the other impinging polarization. This sub-antenna is coupled via a capacitive mechanism to a larger antenna, "CC (capacitive coupling) Antenna," located below on the substrate.

Thermal dissipation (Joule effect) of the incident waves in the resistive loads heats up the thermo-resistive amorphous silicon layer, whose resistance is measured by the read-out circuit. The two antennas couple efficiently to the two linear polarization components of the incident radiation. The membrane is suspended 1-2 µm above a thick (~11 µm) oxide layer covering a metallic reflector. This configuration guarantees at the same time a strong isolation between the detector and the CMOS read-out circuit underneath and a good impedance matching of the antenna over a significant bandwidth. Copper through-oxide vias connect the microbolometer to the read-out circuit through the oxide layer. The pixel size is 50×50 µm and the antennas were optimized to cover the 1-3 THz band. This device is fabricated in LETI's clean room facilities on-top CMOS 8-inch wafers (read-out circuits) provided by a third-party foundry. The micro-bolometer focal plane array (FPA) is mounted inside a vacuum sealed package. A 1mm-thick High-Resistivity Float-Zone Silicon (HRFZ-Si) plate was used as the package window (Fig 1 right).

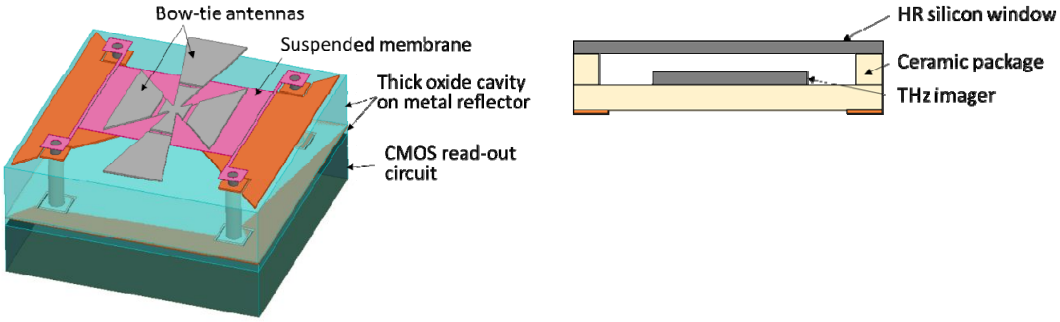

Figure 1. THz microbolometer with double bow-tie antenna (left) and packaging scheme (right).

It is important to point out that similarly to CMOS Field Effect Transistors (FET) or Schottky diodes arrays, bolometer array can reach very-large-scale integration (VLSI) thanks to silicon process technologies. As illustrated by the growing commercial offer of IR bolometer array for consumer applications -for example low cost IR imagers are now sold to be connected to smartphones– this technology applied to THz will benefit from silicon microelectronics assets in terms of yield and cost when applications will emerge.

2.2 Characterized performance of the prototyped LETI arrays

The prototyped 320x240 bolometer arrays targeted the 1-3THz range operation. Spectral responsivity of the imagers has been estimated thanks to an experimental setup based on a Fourier-transform spectrometer [13]. The spectral responsivity of the array is obtained relatively to a calibrated pyroelectric detector with a flat spectral responsivity in the spectral range of interest. From this measurement and from the temporal noise evaluation of the imager in video mode which is close to 350µV RMS, we can assess the spectral minimal detectable power (MDP) of the array.

The figure 2 presents the experimental spectral MDP of the imager for the standard pixel design – design 1 – optimized in the 1-2 THz range. The MDP has also been simulated with the electro-thermal modeling of the detectors coupled to finite element analysis of the spectral response [14]. For comparison, this theoretical MDP is also represented for a broader spectral range. Both simulated and experimental MDP show good agreement.

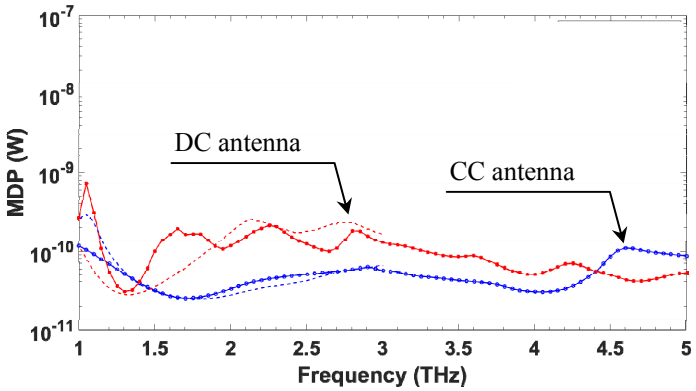

Figure 2. Spectral minimal detectable power (MDP) of the 320x240 THz array –Design 1– for the 2 crossed bow-ties 'CC' & 'DC' antennas (dotted lines : measurement / plain lines: simulated).

A second pixel design – design 2 – with shorter CC antenna has been optimized for higher sensitivity in the 2-3 THz range. Its MDP has been simulated from 1 THz to 5 THz and experimentally confirmed at 2.5 THz by responsivity measurement of the array to the calibrated power of a quantum cascade laser (QCL), operated in a nitrogen dry box covering the whole optical path. As illustrated in figure 3, the measured MDP is very close to the simulated one.

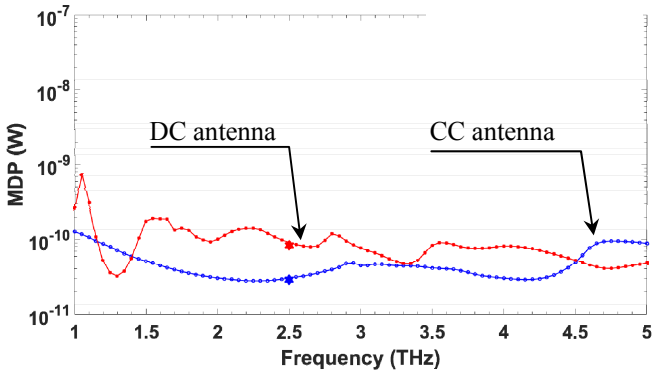

Figure 3. Spectral minimal detectable power (MDP) of the 320x240 THz array –Design 2- for the 2 crossed bow-ties 'CC' & 'DC' antennas (symbol : measurement / plain lines: simulated).

Recently, the performance of the array has been characterized below 1 THz in order to assess the sensitivity out of the optimized spectral range. An optical bench similar to the 2.5 THz validation test has been developed. It comprises an electronic source based on frequency multipliers that covers the 170-1100 GHz range and a calibrated pyroelectric detector to evaluate the impinging power on the array under test.

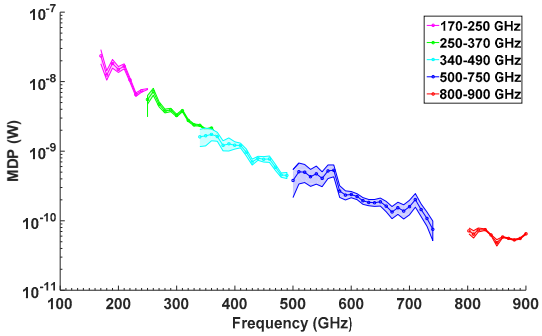

Figure 4. Measured MDP between 0.1 and 1.1 THz of the currently prototyped 320x240 pixel array.

The previous figure presents the experimental MDP values in a range spanning from 170 GHz to 900 GHz. MDP are represented in a ± σ confidence interval due to measurement uncertainties of the power-meter and of the bolometer array

outputs. As previously shown by 3D electro-magnetic (EM) simulations [10], the array presents a resonance at 850 GHz that leads to a MDP better than 50 pW. The MDP increases gradually at lower frequencies but the array still offers pixel-level sensitivity close to 1 nW at 300 GHz.

2.3 Next developments of the THz bolometer arrays technology

This unique approach where the THz radiation absorber (antennas with resistive loads) is separated from the thermometer (amorphous silicon film) offers the flexibility to customize the 2D THz sensor in terms of frequency and polarization sensitivity.

Detection below 1THz is of particular interest for many applications where moderate spatial resolution is needed while absorption in atmosphere and in objects is acceptable. The operation frequency of the detector can be tuned through the antenna dimensions and pitch scaling. However the benefit of keeping the pixel size constant is to keep the same read-out circuit and the same number of pixels on a constant chip area, therefore a cost-effective solution and a high resolution. Current detector sensitivity below 1 THz is limited by the antenna dimensions (50µm long bow ties) and by the thickness of the quarter wavelength dielectric cavity that are optimized for 1-3THz detection.

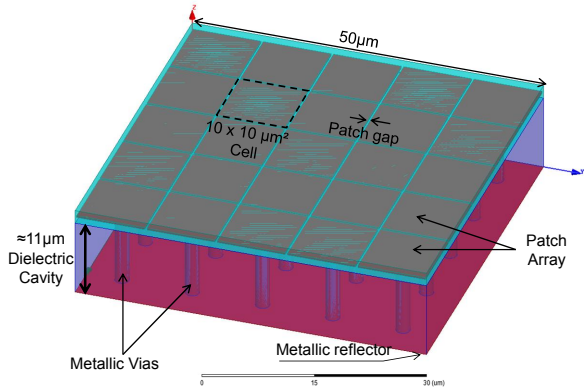

Figure 5. Example of AMC reflector for detection below 1 THz.

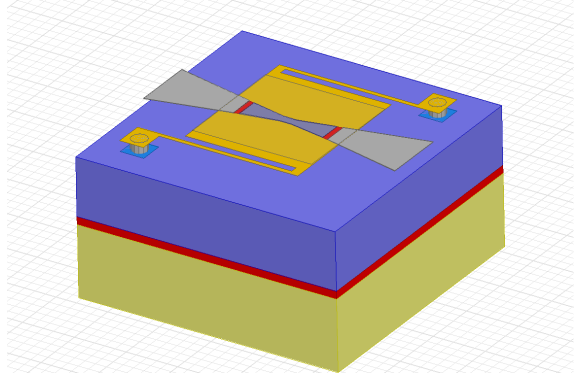
Figure 6. Example of a design with single polarization antenna-coupled THz bolometer.

For future sensors, introduction of AMC (artificial magnetic conductor) within the dielectric cavity will enable efficient detection at lower frequencies without significant changes of pixel design [15]. The AMC consists in Sievenpiper high impedance surfaces (HIS) [16] formed by a patch array connected to the bottom reflector through metallic vias. Monolithic process of such structures at sub-THz frequencies is achieved thanks to prior developments of copper-plugged Through silicon-Oxyde Vias (TOVs) [17]. To cope with the current antenna bolometer design and to maintain the capability of cross-polarization detection, the dielectric slab thickness is fixed to 11 µm and the pitch of symmetric square patch is set smaller than the pixel pitch. The designed pixels (refer to Fig 5) ensure that the gap remains compatible with current lithography capabilities.

With single polarization antenna-coupled pixels, dual polarization imaging can be achieved on the same focal plane array with an alternating arrangement of single polarization pixels so that simultaneous images at each polarization can be delivered in real time by the imager. The pixel pitch being typically below ~λ/2, the spatial resolution of the imager will be limited by the optics. This arrangement will not suffer from a significant degradation of the Modulation Transfer Function (MTF) of the system but will suffer from a reduction in sensitivity as some of the THz radiation will not be collected. A straightforward approach to designing a single polarization pixel (Figure 6) is to remove the CC antenna of the current structure. In this case, the optical coupling is only performed by the DC antenna located on the micro-bolometer membrane.

3. FIELD EFFECT TRANSISTOR ARRAYS TECHNOLOGIES

Two FET-based approaches are developed at LETI: direct detection and heterodyne detection. The former technic has reached the most advanced demonstration with 31x31 arrays and real-time 2D imaging, while the latter has been demonstrated with single-point heterodyne detector and raster scanning at showing very promising sensitivity.

3.1 Direct detection FET-based THz sensor architectures

Although currently proving poorer sensitivities than bolometer THz detectors, FET-based THz direct detection using low-cost CMOS technology appears to be another promising way to realize THz images. Consequently LETI started its work on FET-based THz direct detection sensors in 2008.

Using plasma-wave theory, Dyakonov and Shur theoretically demonstrated [18] [19] in the 1990s that Si-MOSFET may be used as a THz detector. To observe this phenomenon, the MOS transistor is biased by a gate-to-source voltage to which the THz signal is superimposed. Then a small DC voltage is obtained between the drain and the source of the transistor as depicted in figure 7.

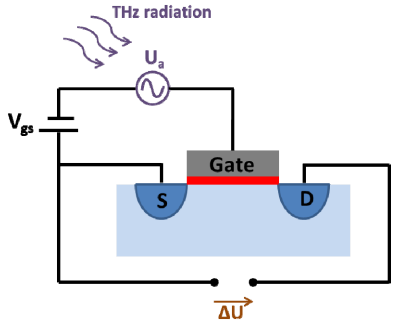

Figure 7. schematic of the THz CMOS detector.

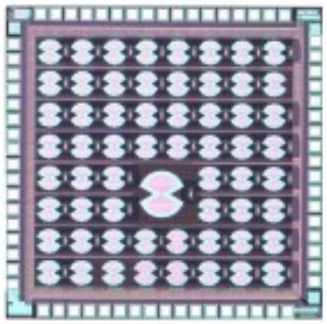

Figure 8. Test chip photograph.

Dyakonov and Shur considered that the FET channel behaves like a 2D electron fluid, in which with particular conditions such as high frequencies, high mobility and short MOS channel, a standing wave can arise. In this case, the MOSFET may be seen as a resonator at the fundamental plasma frequency which delivers high induced drain-to-source voltage. Nevertheless, we made the choice to use a low-cost 0.13µm CMOS process used at room temperature for size, power and cost reasons. Consequently, the mobility in silicon is too low and the MOS channel is too long to obtain resonant conditions, so that the THz signal coupled to the source does not reach the drain due to damping effect. Still, a DC output voltage, proportional to the power of the THz radiation, is detected between drain and source.

Pfeiffer and Roskos groups [20] [21] described the MOSFET-based THz detection using a self-mixing theory and also predicted that the DC drain-to-source voltage is proportional to the squared amplitude of the THz signal present between gate and source. Therefore, antenna gain and efficiency performances directly impact detection quality. Though, always in perspectives of low-cost detectors, above-IC antennas were excluded, forcing the use of CMOS process top metal layers to realize the antenna.

Furthermore, antenna and MOS detector parameters cannot be optimized separately and the impedance matching between the antenna and the MOS detector must be taken into account to obtain an efficient radiation coupling and significant output voltage. LETI [22] designed a bow tie antenna using electromagnetic 3D simulators like ADS Momentum from Agilent and HFSS from ANSYS. This study was concluded by the manufacturing of a test chip (Figure 8) including 61 different pixels which allowed to finely set the optimal parameters for the antenna-MOS detector.

Following this study, LETI developed a pixel array with embedded amplification and signal processing to address the challenges of sensitivity, gain and noise reduction. The signal stemming from the MOS detector is a weak continuous voltage which is consequently prone to high 1/f noise. To overcome this problem, the input THz signal is ON/OFF modulated at a frequency f_{mod} inside the source, modulating the MOSFET output voltage from DC to f_{mod}. The aim of this technique is to move the signal frequency beyond the corner frequency to filter the 1/f noise efficiently. In addition,

the high-Q band-pass filtering provides also thermal noise reduction. In order to realize this selective filtering combined with amplification, LETI implemented a dedicated in-pixel readout architecture [23] which is depicted in the figure 9.

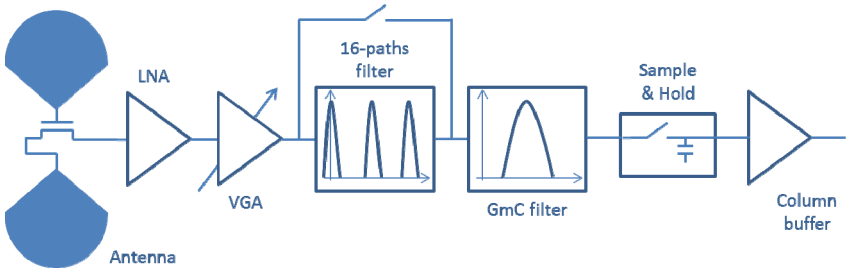

Figure 9. Pixel block diagram.

The first stage of this architecture is an adjustable amplifier including a low noise preamplifier and a variable gain amplifier. The total closed-loop gain may be adjusted from 31dB to 71dB. After this amplification, the signal is demodulated with a high-Q 16-paths switched-capacitors band-pass filter. Furthermore a continuous-time Gm-C filter is inserted to filter out the upper and lower spectral bands generated by the 16-paths filter. The filter central frequency of the N-paths filter and Gm-C filter can be tuned from 75 kHz to 225 kHz in order to match the modulation frequency f_{mod}. A digital sequencer is also implemented in each pixel to generate the control signals and avoid external switching signals routed through the entire array.

The chip was designed in a standard 0.13 µm CMOS process. The whole readout chain, including the antenna and the MOS detector is integrated in a 240x240 μm^2 pixel. The final imager containing a 31x31 pixels array has a total area of 8.5x8.5 mm^2 and allows frame rates from 25 fps up to 100 fps. The total power consumption of one pixel is 210 µW. Picture of the entire chip with a zoomed part is provided in Figure 10.

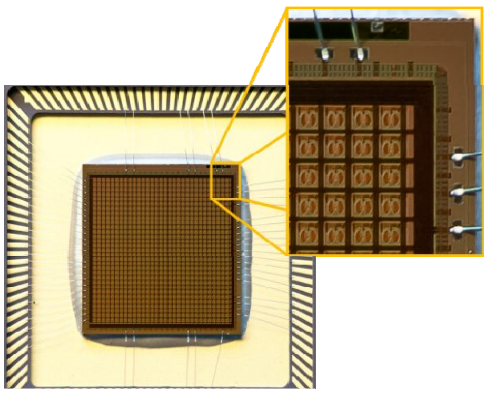

Figure 10. 31x31-pixels FET imager micrograph with zoomed image on the pixels.

3.2 Characterized performance of the prototyped arrays

The 31x31 pixels array was characterized at LETI following the same measurement protocol used for the characterization of the THz bolometer detectors. Thanks to a tunable THz-wave generator, responsivity and sensitivity are measured in a frequency range spanning from 170 GHz to 375 GHz with 10 GHz frequency steps. Furthermore, for each frequency, several measurements are carried out by moving slightly the detector towards the source in order to take into account the stationary wave effect.

Responsivity, mentioned in equation (1), is the ratio of the sum of the pixels output voltages and the THz power beam lighting the imager. Nevertheless, only the pixel output voltages higher than 4 times the rms output noise are summed in order to exclude pixels receiving no THz signal.

$$Rvi_{Freq\ k} = \frac{\sum_{i \in [1;31\times31]}^{V_{pic-pic}>4\sigma} V_{pic-pic,i}}{P_{THz,moy}} \qquad (1)$$

To measure the THz power beam lighting the imager, the detector is replaced by a power-meter and a frequency sweep from 170 GHz to 375 GHz is also realized. Responsivity results are presented in figure 11. Then, the Minimum Detectable Power (MDP), which is the ratio of the output rms noise voltage to the responsivity, is also presented in figure 12.

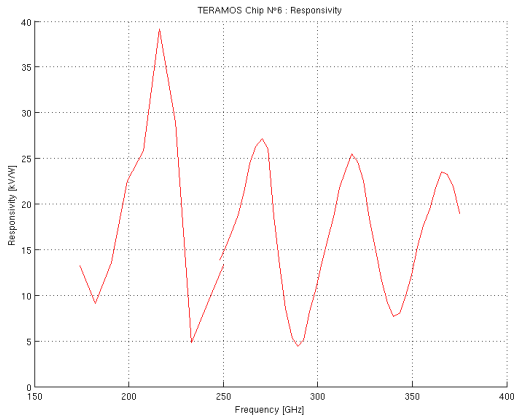

Figure 11. Responsivity.

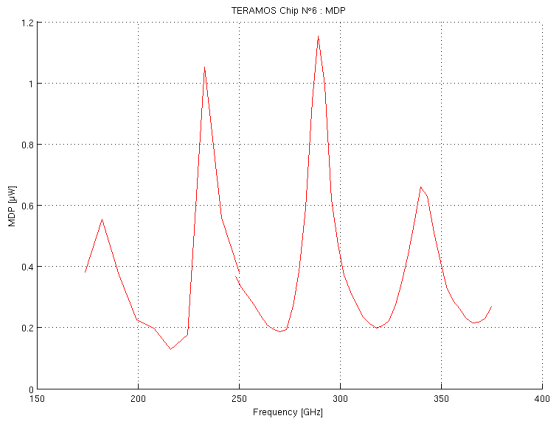

Figure 12. Minimum detectable power.

A video sequence at 100 frames per second using our 31x31 pixels THz has also been performed. For this video, a 200 GHz multiplier chain source is used and its radiation is collimated by an optical lens. The imager is then positioned in the focal plane of a second lens. During the video acquisition a copper ruler is moved in front of the THz beam. The resulting sequence video and the experimental set-up is provided in figure 13.

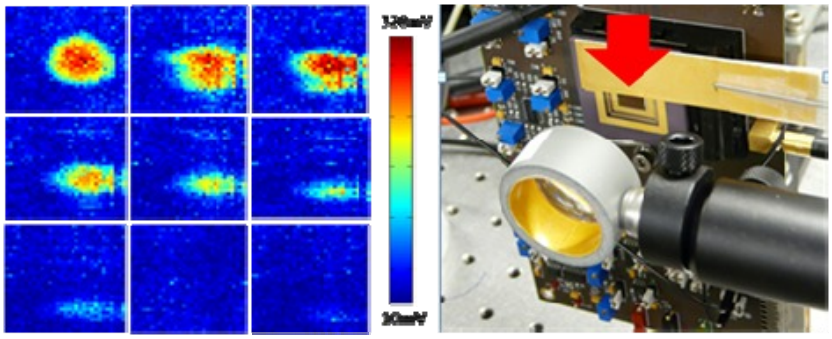

Figure 13. 100 fps sequence of a copper ruler passing in front of a 200 GHz beam.

3.3 Heterodyne detection FET-based THz sensor architectures

The heterodyne detection approach relies on a standard RF receiver that down-converts the RF signal at baseband. Because of the high targeted frequency, the receiver architecture does not include any low noise amplifier after following the integrated antenna, but uses a direct double-side-band mixer. Likewise in the direct detection, the down-conversion is done simply by a passive cold-FET mixer. The main difference is that the RF signal is not mixed on itself, but uses a local oscillator (LO) signal (Figure 14). As shown in figure 14, the conversion gain of the mixer can be increased drastically if the oscillator signal amplitude is high. Besides, the noise figure (NF) is also reduced as it decreases when

the oscillator amplitude increases. Hence, heterodyne architecture for detection offers many advantages since an oscillator signal generated on-chip has naturally higher amplitude than the RF incoming signal. Another advantage is that the Intermediate Frequency (IF) output can be chosen at any baseband frequency for analysis and thus there is no need of modulation at the source side. Finally, a major advantage is that both amplitude and phase can be analyzed with a heterodyne receiver and thereby obtain a vectorial information per pixel.

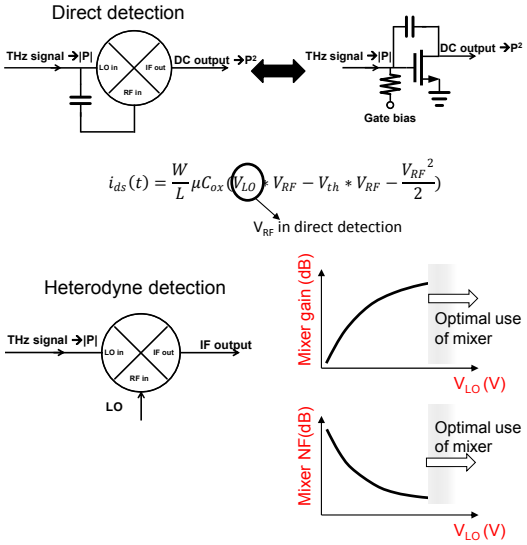

Figure 14. Direct detection and heterodyne detection principle using passive cold-FET mixer

However, heterodyne detection requires an oscillator generating a signal that is usually at higher frequency than the CMOS cut-off frequency. This issue is solved using harmonic extraction techniques where multiple oscillators operate at lower frequency and the components of a specific harmonic are combined at the output (for example the triple-push technique provides the third harmonic). Moreover, the oscillator is injected and locked to a sub-harmonic signal to obtain a stable and low phase noise (PhN) LO signal. Figure 15 shows an example of a CMOS triple-push oscillator with output frequency around 276 GHz and injection frequency at 46 GHz. The resulting output frequency and PhN are determined by the injection signal at 46 GHz.

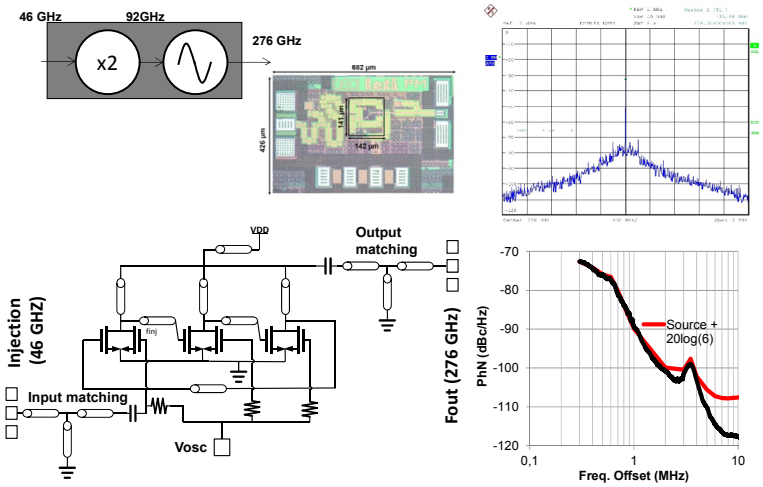

Figure 15. Example of a CMOS 65nm 276 GHz oscillator locked by sub-harmonic injection at 46 GHz.

3.1 Characterized performance of the heterodyne detector

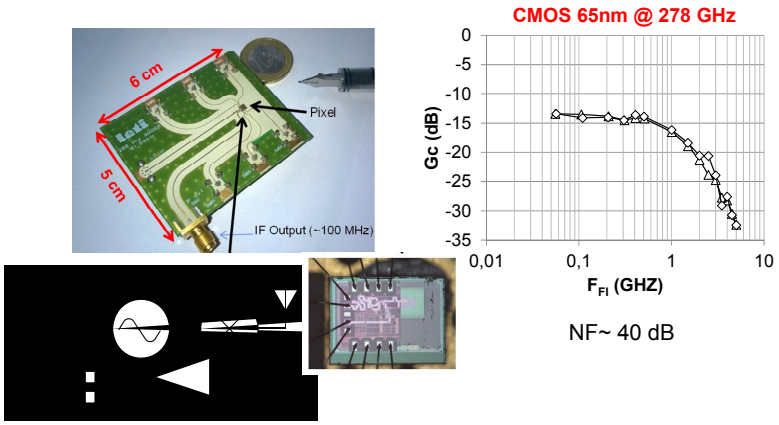

Figure 16. CMOS 65nm 278 GHz heterodyne detector chip and associated conversion gain.

The detector architecture is depicted in figure 16. A single pixel has been fabricated as a prototype in order to demonstrate the operating principle. The circuit operates around 278 GHz and exhibits a conversion gain of -14 dB. The noise figure is 40 dB. The total DC power consumption is 47 mW under 1.2 V supply. The main contributor to the power consumption is the oscillator.

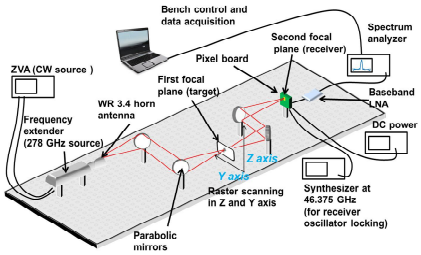

Imager dynamic and noise characteristics						Imaging system
Freq. (GHz)	RBW (KHz)	NF (dB)	Sensitivity (dBm)	Peak power (dBm)	SNR (dB)	Equivalent NEP* (fW/Hz)
278	10	47	-87	-26	61	0.2

*$NEP = K_B T \Delta f F$ with Δf=1Hz, F noise factor [4]

Figure 17. Optical bench using the heterodyne detector and imaging system characteristics. Raster scan image of a dried insect at 278 GHz.

The heterodyne detector prototype has been used for imaging at 278 GHz. Figure 17 shows the optical bench in which the heterodyne detector was placed. This characterization showed that the signal to noise ratio was 61 dB (full dynamic between white and black-noise floor) and a noise figure (NF) of 47 dB. The equivalent NEP is 0.2 fW/Hz.

Raster scan images of a dried insect (megascolia maculata) have been done at 278 GHz. The resulting image was performed with the oscillator locked on a 46.375-GHz injection signal. The image is extracted on a log scale and shows a dynamic range of 50 dB.

4. BOLOMETER VIDEO CAMERA

4.1 Front-end electronics and camera integration

A proximity electronic board was designed to monitor the micro-bolometer array described in sections 2.1-2.2 such as the power supply, synchronizations, video signal, and triggers. The power signal as well as the digitization functions were designed with very low electronic noise (< 5µV RMS in the frequency range 1-10 000 Hz). The video signal is digitized on a 16bit basis.

A second electronic board is used for the USB3 interface: video signal transferring according to USB3 VISION protocol, power supply distributing from the USB3 power supply (5V).

A trigger input/output signal is available. The camera can work as a master and send TTL trigger out or can work as a slave. This function can be used to work in a differential mode: for instance with a THz source with a gate function to make black (source off) reference images. The software interface can show the raw image or the difference image (image – black reference image).

4.2 Design analysis of the optics of the THz camera

A specific terahertz objective lens was designed for this camera (Figure 18). Reaching a f/number as low as possible is important to maximize the sensitivity of the camera. F/numbers of 0.7 to 0.9 are usually achievable in terahertz refractive objective lenses, especially with the use of HRFZ silicon lenses that exhibit a refractive index equal to 3.416 over a wide THz band. HRFZ-Si material has very low internal absorbance. Moreover this material accepts anti-reflective (AR) coatings (one layer of Parylene) in order to avoid reflections at interfaces (~40% per interface). Other THz transparent materials such as TEFLON, HDPE, Zeonex have lower refractive index, and are therefore worse candidates for designing high aperture objective lenses.

The wavelength of 120µm (2.5THz) was chosen for the preferred application of this lens, in order to show good spatial resolution on the objects. The pixel size of 50µm is well adapted for this wavelength, assuming possible F/number lower than 0.9.

According to the preferred identified applications, we designed our lens to have 0.2mm pixel resolution on objects, which leads to a –x0.25 (1/4) magnification (50µm pixel size). At F/0.8, the objective lens has a theoretical cut-off frequency of 10cy/mm (for 120µm wavelength), which is exactly equal to the Nyquist frequency of the focal plane array. This condition leads to well sampled imaging systems, i.e. imaging systems that give higher possible resolution without aliasing.

Figure 18. Camera integrating the 320x240 bolometer array with a specific terahertz objective lens.

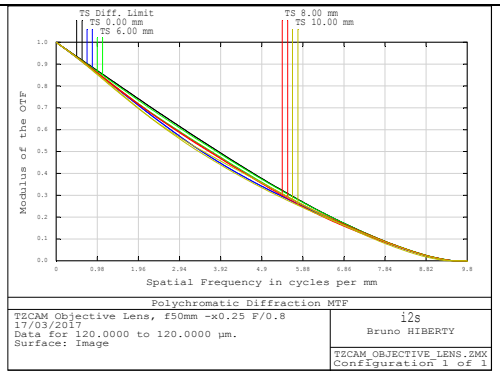

Figure 19. Optical MTF of the TZCAM objective lens @120µm, working distance 196mm.

4.3 Developed optics of the THz camera

The optical design work showed that F/0.8 objective was achievable with 2 HRFZ Si lenses leading to good imaging quality at a distance of 196mm. Lenses are AR coated with parylene, optimized for 120µm. The pupil was chosen to be placed on the front lens to minimize the size and cost of the lenses. Since more than one aspherical surface leads to high

alignment sensitive objective lenses, only one surface is aspherical. Image quality was optimized using MTF criteria, at 5 cy/mm (half cut-off frequency).

At 5cy/mm, theoretical MTF (Figure 19) is better than 90% of the diffraction limit at 120µm wavelength for all field positions of the focal plane array, even when taking into account for manufacturing and misalignment tolerances (tolerancing using Monte-Carlo analysis for more than 80/100 systems). Distortion is lower than 1% over the whole field of view.

Due to the wide transmission range and the constant refractive index of the material, this objective lens has a very large useful spectral bandwidth: 100 GHz – 5THz. If high transmission is needed, AR coatings of the lenses and the image sensor should be optimized for the selected frequency. Although optically optimized for 120µm (2.5THz), this objective lens is still very good for wavelengths down to 60µm (5 THz).

The following table summarizes the optical characteristics of the 50mm –x0.25 magnification f/0.8 at 196mm.

Focal length	50mm
F/number	f/0.8
Useful bandwidth	100Ghz-5 THz
Magnification	x-0.25 @196mm
Optical distortion	<1%
MTF10% frequency	> 7.6 cy/mm
Transmission	> 83% @120µm

5. CONCLUSION AND PERSPECTIVES

Uncooled terahertz (THz) real-time imaging cameras with two-dimensional (2D) sensors are expected to address a wide range of applications in industrial, medical, and security markets. For many years, LETI has been developing promising technologies to meet the low cost and low SWAP (Size, Weight, And Power) requirements of these applications based on bolometer and CMOS technologies, which are both compatible to standard silicon microelectronics processes.

A 320x240 bolometer array has been developed for the 1-3 THz frequency range with MDP values lower than 100 pW; the maturity and state-of-the-art sensitivity of this sensor led to the development of a commercial real-time THz camera with a f/0.8 optics showing high MTF and good transmission.

FET detectors offer lower cost alternatives in the sub-THz range and a 31x31-pixels sensor has been developed. This sensor includes a configurable signal processing chain embedded in each pixel of the array for direct detection, amplification and filtering, thereby dramatically reducing the noise.

Finally, single-pixel heterodyne source and detector have been designed and prototyped with preliminary demonstrations of highly sensitive raster scanning THz imaging.

Future developments of these complementary uncooled THz imaging technologies suitable for active real-time imaging will target sensitivity improvement of bolometer arrays in the sub-THz range, optimized optical coupling of direct-detection FET arrays, and multi-pixel heterodyne FET detectors for fast image acquisition.

ACKNOWLEDGEMENTS

The support from CEA as well as from the EU FP7 project MUTIVIS is gratefully acknowledged. The authors also acknowledge the LETI team and academic institutions –in France, University of Savoie, University of Paris 7, IEMN, University of Rennes, Ecole Normale Supérieure de Paris- for their fruitful collaborations.

Special thanks to the DGA for their financial support.

REFERENCES

[1] F. Simoens, "Handbook of Terahertz Technologies: Devices and Applications" chapter "THz cameras", edited by Ho-Jin Song & Tadao Nagatsuma, by Pan Stanford, ISBN 9789814613088, April 15, (2015).
[2] i2S, http://www.i2s.fr/project/camera-terahertz-tzcam/
[3] NEC, http://www.nec.com/en/global/prod/terahertz/
[4] INO, http://www.ino.ca/en/products/terahertz-camera-microxcam-384i-thz/
[5] TicWave, http://ticwave.com/products.html
[6] Terasense, http://terasense.com/products/sub-thz-imaging-cameras/
[7] Nethis, http://nethis-thz.com/index.php/openview/
[8] Ophir, http://www.ophiropt.com/laser--measurement/beam-profilers/products/Beam-Profiling/Camera-Profiling-with-BeamGage/Pyrocam-IV
[9] Yon J-J., Mottin E., Tissot J.L., "Latest amorphous silicon microbolometer developments at LETI-LIR," Proc. SPIE 6940, 6940-61 (2008).
[10] Simoens F., Meilhan J., Nicolas J-A., "Terahertz Real-Time Imaging Uncooled Arrays Based on Antenna-Coupled Bolometers or FET Developed at CEA-LETI," J. Infrared Millimeter Terahertz Waves 36, 961–985 (2015).
[11] Simoens F. et al., "Real-time imaging with THz fully-customized uncooled amorphous-silicon microbolometer focal plane arrays," Proc. SPIE 8363, 83630D–83630D–12 (2012).
[12] Simoens F., Meilhan J., "Terahertz real-time imaging uncooled array based on antenna- and cavity-coupled bolometers," Philosophical Transactions of the Royal Society of London A: Mathematical, Physical and Engineering Sciences 372(2012), 20130111 (2014).
[13] Nguyen D.T., Simoens F., Ouvrier-Buffet J.-L., Meilhan J., Coutaz J.-L., "Simulations and Measurements of the Electromagnetic Response of Broadband THz Uncooled Antenna-coupled Microbolometer Array," IEEE Transactions on Terahertz Science and Technology 2(3), 299 – 305 (2012).
[14] Meilhan J., Oden J., Ouvrier-Buffet J.L., Hamelin A., Delplanque B., and Simoens F., "Uncooled terahertz video micro-bolometer camera: Toolbox to optimize the sensitivity by tuning antennas and cavity," IRMMW-THz, (2016).
[15] J-L. Ouvrier-Buffet, U.S. Patent 2013/0146773 Al, June 13, (2013).
[16] Sievenpiper D. et al., "High-impedance electromagnetic surfaces with a forbidden frequency band," IEEE Transactions on Microwave Theory and Techniques 47(11), 2059–2074 (1999).
[17] Pocas S et al., "Technological customization of uncooled amorphous silicon microbolometer for THz real time imaging," Proc. SPIE 8624, 862419 (2013).
[18] Dyakonov M. & Shur M., "Detection, mixing, and frequency multiplication of terahertz radiation by two-dimensional electronic fluid," IEEE Transactions on Electron Devices 43(3), 380–387 (1996).
[19] Dyakonov M. & Shur M., "Shallow water analogy for a ballistic field effect transistor: New mechanism of plasma wave generation by dc current," Phys. Rev. Lett. 71(15), 2465–2468 (1993).
[20] Pfeiffer U. R., Ojefors E., Lisaukas A., Glaab D., and Roskos H. G., "A CMOS focal-plane array for heterodyne terahertz imaging," IEEE Radio Frequency Integrated Circuits Symposium, 433–436 (2009).
[21] Ojefors E., Pfeiffer U. R., Lisauskas A., and Roskos H. G., "A 0.65 THz Focal-Plane Array in a Quarter-Micron CMOS Process Technology," IEEE Journal of Solid-State Circuits 44(7), 1968–1976 (2009).
[22] Schuster F., Videlier H., Dupret A., Coquillat D., Sakowicz M., Rostaing J., Tchagaspanian M., Giffard B., and Knap W., "A broadband THz imager in a low-cost CMOS technology," IEEE Int. Solid-State Circuits Conference (ISSCC), 42–43 (2011).
[23] A. Boukhayma, J-P. Rostaing, A. Mollard, F. Guellec, M. Benetti, G. Ducournau, J-F. Lampin, A. Dupret, C. Enz, M. Tchagaspanian, J-A. Nicolas, "A 533pW NEP 31×31 pixel THz image sensor based on in-pixel demodulation," IEEE European Solid State Circuits Conference (ESSCIRC), 303-306 (2014).